

Double-periodic blue variables in the Magellanic Clouds

R.E. Mennickent¹ G. Pietrzyński^{1,2} M. Diaz³ W. Gieren¹

¹ Universidad de Concepción, Departamento de Física, Casilla 160-C, Concepción, Chile
e-mail: rmennick@stars.cfm.udec.cl, pietrzyn@hubble.cfm.udec.cl, wgieren@coma.cfm.udec.cl

² Warsaw University Observatory, Al. Ujazdowskie 4,00-478, Warsaw, Poland

³ Instituto Astronômico e Geofísico, Universidade de São Paulo, Brazil
e-mail: marcos@astro.iag.usp.br

Abstract. We report the discovery, based on an inspection of the OGLE-II database, of a group of blue variables in the Magellanic Clouds showing simultaneously two kinds of photometric variability: a short-term cyclic variability with typical amplitude $\Delta I \sim 0.05$ mag and period P_1 between 4 and 16 days and a sinusoidal, long-term cyclic oscillation with much larger amplitude $\Delta I \sim 0.2$ mag with period P_2 in the range of 150-1000 days. We find that both periods seems to be coupled through the relationship $P_2 = 35.2 \pm 0.8 P_1$. In general, the short term variability is reminiscent of those shown by Algol-type binaries. We propose that the long-term oscillation could arise in the precession of a elliptical disc fed by a Roche-lobe filling companion in a low mass ratio Algol system.

Key words. stars: binaries: eclipsing - stars: binaries: close - stars: variable: general - stars: early-type

1. Introduction

Over the past years, the microlensing projects (OGLE, MACHO, EROS) have monitored millions of stars in the Magellanic Clouds and Galactic bulge for variability. The resulting huge photometric databases are very well suited not only for microlensing studies but also for many other issues of modern astrophysics, including the distance scale, variable stars, star clusters etc. In particular, the OGLE-II project (Udalski, Kubiak and Szymanski, 1997), has provided accurate BVI measurements for about 6.5 million stars from the central parts of the Magellanic Clouds (Udalski et al. 1998, 2000). Based on this same material, a unique catalog containing about 68.000 variable stars has just been released (Żebruń et al. 2001).

One example of the scientific information that it is possible to extract from such a catalogue is shown by the work of Mennickent et al. (2002, hereafter M02), who report the discovery of Be star candidates in the Small Magellanic Cloud showing unexpected photometric variations. Basically, these authors found four types of variability in targets within the luminosity-colour box of typical Be stars: Type-1 stars showing outbursts, Type-2 stars showing sudden magnitude jumps, Type-3 stars showing periodic variations and Type-4 stars showing random variability. According to these authors, possible causes for Type-1 and Type-2 stars include blue pre-main sequence stars surrounded by thermally unstable accretion discs and white dwarfs accreting from the Be star envelope in a Be+WD binary. Type-4 stars could be classical Be stars.

On the other hand, Type-3 stars could not be linked to the Be star phenomenon at all, mainly due to their rather red colours and strictly periodic behaviour. The above study is complemented by the work by Keller et al. (2002) on blue variable stars from the MACHO database in the LMC. These authors report basically the same photometric behaviour in a sample of LMC blue variables. These authors also find emission lines in the spectra of many of these variables.

Further inspection of the mysterious Type-3 stars found in the SMC and the LMC (Mennickent et al. in preparation) revealed 30 objects showing double-periodic photometric variations: a long-period sinusoidal variation and a short-period modulation. Some of these short-term light curves are typical of eclipsing Algol variables. The study of this new double-period photometric variability is the subject of this paper.

2. Light curve analysis and the long-term oscillation

Table 1 lists the Type-3 stars in the SMC and LMC where two photometric periods were found while Fig.1 shows some examples of light curves. MACHO light curves were also inspected to confirm the long-term variations and search for colour variability. MACHO identifications are also provided along with the OGLE-II names in Table 1. In general, the long-term periodicity was evident from the first inspection of the light curve. The period P_2 in these cases was calculated using algorithms based on

the F (variance ratio) statistics and fourier transform giving consistent results. The results shown in Table 1 reveal that the long-term variations have periods between 140–960 d. The period error was calculated as the half width at half maximum of the periodogram peak. Trial and error tests showed that these are upper limits for the error and the accuracy of P_2 in Table 1 is likely better than shown by a factor 2 at least. After finding P_2 , we applied a non-linear least squares fit to the data of the type:

$$I = I_0 - A_I \sin(2\pi(HJD - HJD_0)/P_2) \quad (1)$$

where I_0 , A_I and HJD_0 were parameters to be determined while the period P_2 remained fixed. The half-amplitudes A_I found were between 0.03 and 0.26 mag. The residuals to the best fit were examined with the same period searching routines employed for the analysis of the long-term oscillation. The surprising result was that in all cases listed in Table 1 we find a second period P_1 , in the range of 2–16 days, which is listed along with their error in Table 1. For non-eclipsing stars this error was found in the same way that for P_2 , but for 5 eclipsing stars the accuracy was usually much better and the error was estimated interactively.

We also studied the MACHO data for all the variables in our sample, constructing the b , r and $b - r$ light curves, and searched for periodicities. We confirmed the periods found on the basis of the OGLE-II database, and found that for all cases the long-term oscillation is redder at maximum (Fig. 2). In general, the colour variations are of very low amplitude (Table 1).

3. On the short-term light curves

Once the long-period sinusoidal modulation is subtracted, the phase curve of the residuals (Fig. 1) turned out to be of three types: eclipsing, double-wave and single-wave. The light curve of the eclipsing stars are typical of those found in Algol type variables. On the other hand, the fact that the stars showing double-wave or single-wave light curve share similar long-term variability with the eclipsing stars and exhibit similar correlation between the short-term and long-term period (see next section) suggests that we are in presence of an homogenous group of short-period variables, and that these non-eclipsing stars could also be Algol-like stars but seen under higher orbital inclinations. The period range along with the fact that emission lines have been observed in Type-3 stars (M02 and Keller et al. 2002) are consistent with this interpretation. In this view, double-wave light curves arises from the changing aspects of a non-spherical Roche-lobe filling secondary star, as occurs in the suspected Algol-type binary V 1080 (Simon et al. 2000). It is worth to mention that long-term periodic oscillations have been reported in a few Algol systems but with very low amplitude (e.g. Walter 1981). The fact that Algols contain B-A type primaries and cooler secondaries should explain the distribu-

tion of Type-3 stars in their colour-colour diagram (M02). In 5 cases we found single-wave light curves. It is possible that the true period is twice the reported period in these cases. This is confirmed by the similar power shown by P_1 and $2 \times P_1$ in the periodogram and also by the good fit of $2 \times P_1$ by the $P_1 - P_2$ linear correlation (see next section).

4. The $P_2 - P_1$ relationship

In Fig. 3 we show what we consider the most surprising result of this paper. The P_2 and P_1 periods seems to be correlated. All five deviant points correspond to single-wave light curves, so it is possible that the true orbital period has been missed by a factor 2. The value $2 \times P_1$ is also indicated in the figure. A linear least squares fit passing by zero gives:

$$P_2 = 35.17(75)P_1 \quad (2)$$

with a correlation coefficient 0.97 and standard deviation of 28 days. The existence of such a relationship suggests that the phenomenon causing the long-term oscillation could be directly related to the binary nature of the system.

5. Discussion: on the nature of the long-term oscillation

The long-term well behaved sinusoidal modulations observed in our sample is not known to occur in other types of blue variable stars. Here we propose as a possible cause for the long-term oscillation the precession of an elliptical disc around a blue star in a semi-detached binary system. The origin of the disc ellipticity and precession could be the tidal interaction between the disc and the Roche-lobe filling secondary star, in a similar way that occurs in short-orbital period dwarf novae of the SU UMa class during superoutburst (e.g. Patterson 2001).

The 3:1 resonance between a disc particle orbiting the primary and the binary system occurs at $R_{disc} \approx 0.46a$, where a is the binary separation. Elliptical orbits at this radius will experience a dynamical apsidal advance with a period given by:

$$P_p = \frac{\sqrt{1+q}}{0.37q} (R_{disc}/0.46a)^{-2.3} P_o \quad (3)$$

(Murray 2000) where q is the ratio between the mass of the secondary star and the primary star and P_o the orbital period. If we interpret P_1 as the orbital period and P_2 as the precession period, then the above equation imposes a strong correlation between both periodicities, as effectively seen in Fig. 3. The observed slope of $P_2/P_1 \approx 35$ should imply a mass ratio $q \approx 0.08$ for $R_{disc} = 0.46a$. There are few Algols with $q < 0.1$ (e.g. Richards & Albright 1999), and they do not show the long-term oscillations described in this paper. However it is exciting that only in these low q systems two important conditions are fulfilled: the primary radius is smaller than the

Table 1. The double-periodic blue stars. OGLE name and MACHO identification are given for every star, along with their photometric period and error. The half amplitude of the long-term variation is also given for the OGLE I band and the MACHO b band, along with the epoch (HJD–2 400 000) for the faint-to-bright mean level crossing for the MACHO b band. The half amplitude of the MACHO $b-r$ light curve is also given, along with their difference in phase with the b curve, considering the epoch for positive to negative mean $b-r$ level crossing as reference. Dashes indicate non-detected or marginal colour variations. A note indicates the appearance of the short-term variability: double-wave (dw), single wave (sw) or eclipsing with two minima (e).

| Star | MACHO ID | P_1 (d) | P_2 (d) | A_I | A_b | E_b | A_{b-r} | $\Delta\Phi$ | Note |
|----------------------|---------------|------------|-----------|-------|-------|------------|-----------|--------------|------|
| OGLE00451755-7323436 | 212.15675.158 | 5.178(5) | 171(15) | 0.12 | 0.11 | 50350.2(8) | 0.02 | -0.35 | dw |
| OGLE00474820-7319061 | 212.15847.466 | 5.497(7) | 177(10) | 0.12 | 0.10 | 50329.3(7) | - | - | dw |
| OGLE00553643-7313019 | 211.16304.169 | 5.092(5) | 176(17) | 0.08 | 0.04 | 50238(1) | 0.02 | 0.53 | dw |
| OGLE05025323-6909493 | 1.3686.53 | 8.025(18) | 255(30) | 0.17 | - | - | - | - | dw |
| OGLE05040378-6917508 | 1.3805.130 | 6.223(7) | 207(20) | 0.11 | - | - | - | - | dw |
| OGLE05060009-6855025 | 1.4174.42 | 3.849(7) | 230(22) | 0.19 | - | - | - | - | sw |
| OGLE05101621-6854290 | 79.4900.185 | 4.301(6) | 319(34) | 0.06 | 0.04 | 50344(2) | 0.02 | 0.53 | sw |
| OGLE05115466-6846369 | 2.5144.4555 | 9.138(2) | 361(29) | 0.26 | - | - | - | - | e |
| OGLE05142677-6910559 | 79.5501.400 | 6.515(2) | 224(14) | 0.13 | 0.08 | 50430(2) | 0.04 | -0.43 | e |
| OGLE05143758-6852259 | 79.5506.139 | 5.372(6) | 185(11) | 0.14 | 0.10 | 50237.3(5) | 0.03 | 0.55 | dw? |
| OGLE05152654-6923257 | 79.5740.5092 | 6.292(8) | 205(15) | 0.04 | 0.04 | 50275.3(6) | - | - | dw |
| OGLE05155332-6925581 | 79.5739.5807 | 7.2835(16) | 188(11) | 0.11 | 0.08 | 50254(1) | 0.03 | 0.54 | e |
| OGLE05171401-6936374 | 78.5979.58 | 8.309(4) | 311(21) | 0.13 | 0.08 | 50345(1) | 0.03 | 0.48 | e |
| OGLE05194110-6931171 | 78.6343.81 | 6.9044(10) | 226(13) | 0.11 | 0.06 | 50247(2) | 0.02 | 0.59 | e |
| OGLE05195898-6917013 | 80.6468.83 | 2.410(10) | 140(5) | 0.06 | 0.04 | 50267.6(8) | - | - | sw |
| OGLE05203325-6910146 | 80.6469.95 | 5.737(5) | 182(10) | 0.04 | 0.05 | 50357.1(8) | - | - | dw |
| OGLE05260516-6954534 | 77.7426.140 | 3.632(3) | 233(15) | 0.07 | 0.07 | 50425.7(7) | - | - | sw |
| OGLE05274332-6950556 | 77.7669.1013 | 7.320(11) | 227(20) | 0.05 | 0.03 | 50280(1) | 0.02 | 0.54 | dw |
| OGLE05285370-6952194 | 77.7911.26 | 15.854(31) | 620(70) | 0.07 | 0.06 | 50388(2) | 0.01 | 0.67 | dw |
| OGLE05294913-6949103 | 77.8033.140 | 7.184(8) | 258(20) | 0.10 | 0.09 | 50382.2(6) | 0.01 | -0.38 | dw |
| OGLE05295881-6934075 | 77.8036.5142 | 5.597(4) | 179(8) | 0.12 | - | - | - | - | dw |
| OGLE05313130-7012584 | 7.8269.36 | 9.231(21) | 960(176) | 0.04 | 0.03 | 51226(4) | - | - | sw |
| OGLE05333926-6956229 | 81.8636.51 | 7.863(15) | 257(18) | 0.03 | 0.01 | 50335(2) | 0.01 | 0.52 | dw |
| OGLE05371342-7010580 | 11.9237.2121 | 10.913(23) | 421(40) | 0.12 | - | - | - | - | dw |
| OGLE05390681-7027487 | 11.9475.96 | 6.967(12) | 276(15) | 0.10 | 0.01 | 50335(2) | 0.01 | 0.52 | dw |
| OGLE05390992-7019262 | 11.9477.138 | 6.632(8) | 198(15) | 0.10 | 0.05 | 50301(1) | 0.02 | 0.56 | dw |
| OGLE05391746-7044019 | 11.9592.22 | 7.151(8) | 219(20) | 0.06 | 0.04 | 50401.0(8) | 0.01 | -0.49 | dw |
| OGLE05410217-7011043 | 76.9842.2444 | 7.352(13) | 264(26) | 0.11 | 0.11 | 50395(2) | - | - | dw |
| OGLE05410942-7002215 | 76.9844.110 | 6.586(9) | 245(23) | 0.12 | 0.09 | 50510(2) | - | - | dw |
| OGLE05435003-7057431 | 15.10314.144 | 5.012(5) | 173(12) | 0.12 | 0.09 | 50250.7(7) | - | - | dw |

stream circularization radius, being possible the formation of an accretion disc (e.g. Richards & Albright 1999) and the 3:1 resonance radius is below the tidal truncation radius, so the disc could in principle grown beyond the 3:1 resonance and may eventually start to precess (Fig. 4). Long-term spectroscopic observations and detailed modeling are required to confirm this scenario.

Acknowledgements. REM acknowledges support by Grant Fondecyt 1000324 and DI UdeC 202.011.030-1.0. MPD thanks CNPq support under grant # 301029. We thank the OGLE collaboration team for making their data public domain. This paper also utilizes public domain data originally obtained by the MACHO Project.

References

Keller, S.C., Bessell, M.S., Cook, K.H., Geha, M. & Syphers, D. 2002, *ApJ*, 124, 2039

Mennickent, R. E., Pietrzyński, G., Gieren, W., & Szewczyk, O. 2002, *A&A*, 393, 887
Murray, J.R. 2000, *MNRAS*, 314, L1
Patterson, J. 2001, *PASP*, 113, 736
Richards, M.T. & Albright, G.E. 1999, *ApJS*, 123, 537.
Šimon, V., Hanžl, D., Škoda, P., & Gális, R. 2000, *A&A*, 360, 637
Udalski, A., Kubiak, M., & Szymanski, M. 1997, *Acta Astronomica*, 47, 319.
Udalski, A., Szymanski, M., Kubiak, M., et al. 1998, *Acta Astron.*, 48, 147
Udalski, A., Szymanski, M., Kubiak, M., et al. 2000, *Acta Astron.*, 50, 307
Walter, K. 1981, *A&A*, 101, 369
Warner, B. 1995, *Cataclysmic Variable Stars*, Cambridge Astrophysics Series 28, Cambridge University Press
Żebruń, K., Soszynski, I., Wozniak, P. R., et al. 2001, *Acta Astron.* 51, 317

Figure Captions

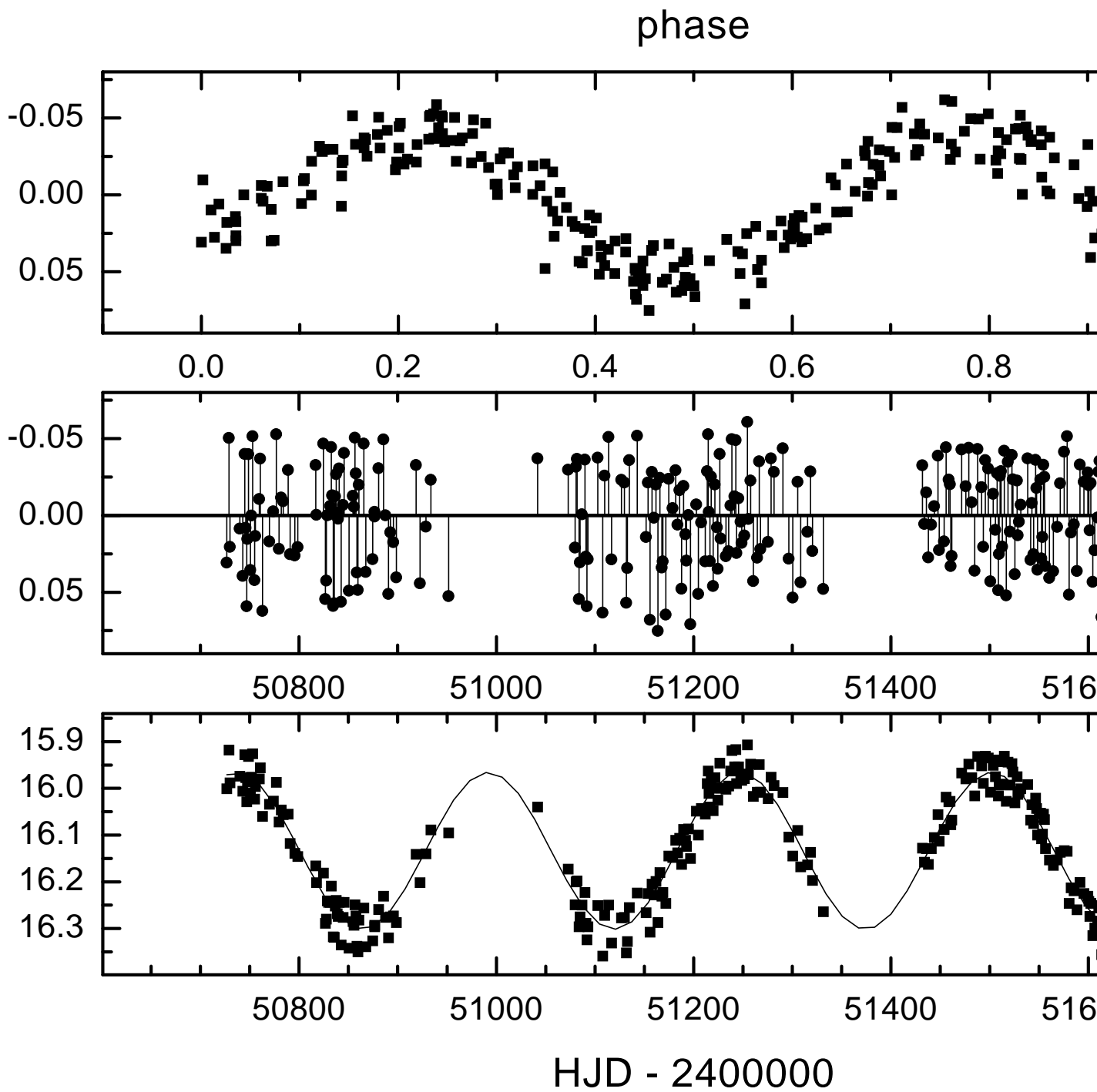
Fig. 1: Eclipsing (upper graph) and double-wave (below graph) light curves. The three pannels in every graph show, from bottom to top, the long-term light variability, the residuals from a sinusoidal fitting and the residuals folded using the short-term period.

Fig. 2: MACHO b and $b - r$ light curves folded with the long-term period.

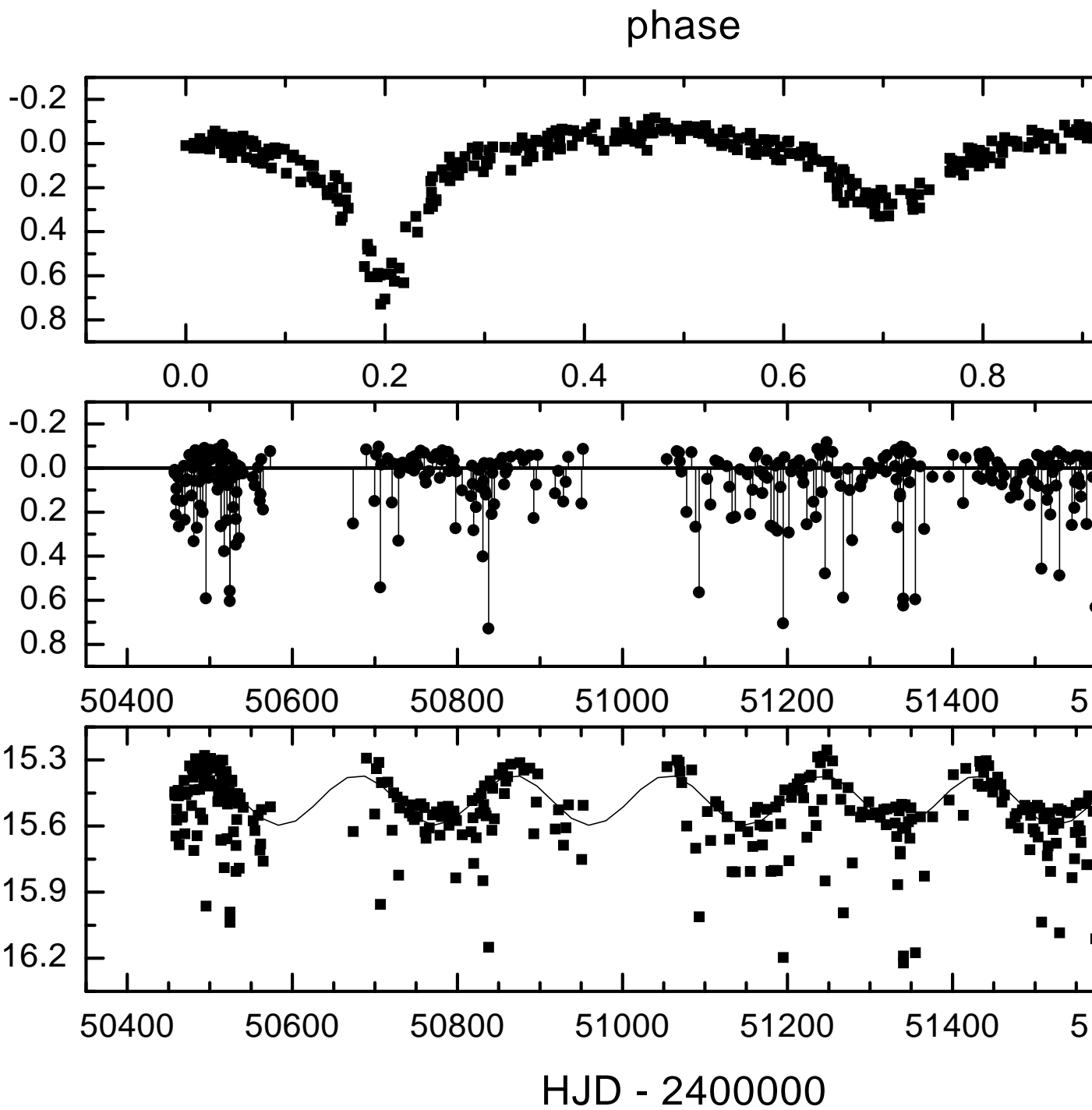
Fig. 3: The long-term period P_2 versus the short-term period P_1 . The errors in P_1 are smaller than the used symbols. Dashed horizontal lines connect two possible solutions for stars with single-wave short-term light curve. The linear fit given by Eq.(2) is also shown.

Fig. 4: The primary radius in units of the the binary separation for the Algols shown by Richards & Albright 1999 (filled circles). The circularization radius, the tidal truncation radius and the 3:1 resonance radius, all of them in units of the binary separation, are shown as a function of the mass ratio. Theoretical expressions for these quantities have been taken from Warner (1995). It is possible that only Algols with very low mass ratios could maintain (precessing) accretion discs beyond the 3:1 resonance.

OGLE 5025323-6909493



OGLE 05155332-6925581



MACHO ID 79.5506.139

